Anterior and Posterior Optic Nerve Head Blood Flow in Nonhuman Primate Experimental Glaucoma Model Measured by Laser Speckle Imaging Technique and Microsphere Method

Lin Wang, Grant A. Cull, Chelsea Piper, Claude F. Burgoyne, and Brad Fortune

Purpose. To characterize optic nerve head (ONH) blood flow (BF) changes in nonhuman primate experimental glaucoma (EG) using laser speckle flowgraphy (LSFG) and the microsphere method and to evaluate the correlation between the two methods.

Methods. EG was induced in one eye each of 9 rhesus macaques by laser treatment to the trabecular meshwork. Prior to lasering and following onset of intraocular pressure (IOP) elevation, retinal never fiber layer thickness (RNFLT) and ONH BF were measured biweekly by spectral-domain optical coherence tomography and LSFG, respectively, until RNFLT loss was approximately 40% in the EG eye. Final BF was measured by LSFG and by the microsphere method in the anterior ONH ($MS\text{-}BF_{ANT}$), posterior ONH ($MS\text{-}BF_{POST}$), and peripapillary retina ($MS\text{-}BF_{PP}$).

Results. Baseline RNFLT and LSFG-BF showed no difference between the two eyes ($P = 0.69$ and $P = 0.43$, respectively, paired *t*-test). Mean (±SD) IOP was 30 ± 6 mm Hg in EG eyes and 13 ± 2 mm Hg in control eyes ($P < 0.001$). EG eye RNFLT and LSFG-BF were reduced by 42 ± 16% ($P < 0.0001$) and 22 ± 13% ($P = 0.003$), respectively, at the final time point. EG eye $MS\text{-}BF_{ANT}$, $MS\text{-}BF_{POST}$, and $MS\text{-}BF_{PP}$ were reduced by 41 ± 17% ($P < 0.001$), 22 ± 34% ($P = 0.06$), and 30 ± 12% ($P = 0.001$), respectively, compared with the control eyes. Interocular ONH LSFG-BF differences significantly correlated to that measured by the microsphere method ($R^2 = 0.87$, $P < 0.001$).

Conclusions. Chronic IOP elevation causes significant ONH BF decreases in the EG model. The high correlation between the BF reduction measured by LSFG and the microsphere method provides evidence that the LSFG is capable of assaying BF for a critical deep ONH region. (*Invest Ophthalmol Vis Sci.* 2012;53:8303–8309) DOI:10.1167/iovs.12-10911

From the Devers Eye Institute, Legacy Research Institute, Portland, Oregon.

Supported by National Eye Institute/National Institutes of Health Grants R01-EY019939 (LW), R01-EY011610 (CFB), and R01-EY019327 (BF); Legacy Good Samaritan Foundation, Portland, Oregon; and unrestricted research fund from Pfizer, Inc.

Submitted for publication September 5, 2012; revised November 5, 2012; accepted November 12, 2012.

Disclosure: **L. Wang**, None; **G.A. Cull**, None; **C. Piper**, None; **C.F. Burgoyne**, None; **B. Fortune**, None

Corresponding author: Lin Wang, Devers Eye Institute, Legacy Health, 1225 NE 2nd Avenue, Portland, OR, 97232; lwang@deverseye.org.

Glaucoma remains a major cause of blindness around the world, yet the sequence of pathophysiologic events defining its etiology remains unknown. Although elevated intraocular pressure (IOP) is one of the major risk factors, impaired microcirculation, particularly in the optic nerve head (ONH), may contribute to initiation and progression of glaucoma. However, despite a number of studies that have demonstrated reduced blood flow (BF) in the glaucomatous ONH,[1–4] the exact role of hemodynamic changes associated with the pathologic mechanisms in glaucoma remains obscure due partially to the complexity of the ONH blood supply, its unique regulatory mechanisms, and limitations of the technologies used for ONH BF measurement.[5–7]

BF in the ONH is supplied by two arterial systems.[8,9] The superficial nerve fiber layer (NFL) is supplied principally by the central retinal artery (CRA); the prelaminar, laminar, and retrolaminar layers are supplied by ciliary arteries (CAs). Physiologically, BF regulatory mechanisms may also differ across these regions supplied by these two vascular systems due to differences in their autonomic innervations.[10,11] It has also been proposed that it is the deep ONH region supplied by ciliary arteries that is associated with pathologic changes in glaucoma.[6,12] However, the most current techniques available for BF measurement, particularly the optically based techniques, such as laser Doppler flowmetry, are thought to measure principally the most superficial tissue supplied by CRA (i.e., the NFL in the ONH surface).[6] Contributions to the measurement from deeper layers supplied by the CAs may vary depending on the techniques and tissue properties.[13–16] It becomes even more complicated when BF is measured in patients with significant NFL thinning, such as glaucoma. In these patients, BF from tissues that are otherwise normally too deep to reach using such measures may begin to contribute to the measured BF.[17] Thus, application of optically based, in vivo modalities for ONH BF measurement in glaucoma is limited by lack of knowledge about the BF in deep tissues of the ONH, its relative contribution to measurement made by various modalities, and its possible alteration in glaucoma.

The microsphere method is an invasive terminal method for BF measurement that can be applied to virtually all tissues of the body if the tissue volume is sufficiently large to accommodate adequate numbers of microspheres. Because the microsphere method measures actual BF, it has often been used to validate BF measurements made using other techniques.[18–20] One particular advantage of the microsphere technique is the capability it provides to measure ONH BF within specific layers.[21]

In the current study, ONH BF in a nonhuman primate model of experimental glaucoma (EG) based on chronic unilateral IOP elevation was determined by both a laser speckle flowgraphy (LSFG) device and the microsphere method, which measures

Copyright 2012 The Association for Research in Vision and Ophthalmology, Inc.

BF within specifically defined depth regions of the ONH. Although the LSFG has been used in clinical settings and in experimental animals to assess ocular hemodynamics,[22–26] there are concerns that variations in the optical properties of different ocular tissues and variations in those properties due to the transition from normal to a pathologic state, may affect the absorbance and scattering of the laser source, potentially confounding BF estimates made by LSFG (and other optical techniques).[27] Comparing the BF measurement between the two methods may provide insight into how ONH BF changes in EG and validate ONH BF measurements made by LSFG, an emerging in vivo optical technique.

The purpose of the current study was therefore twofold. First, was to characterize ONH blood flow change at approximately 40% retinal nerve fiber layer thickness (RNFLT) loss in the EG model. Second, was to compare and correlate the BF measurements by LSFG and the microsphere method.

Methods

Animals and Anesthesia

Nine adult rhesus monkeys (*Macaca mulatta*) were included in the study (7 females, 2 males; 9.7 ± 3.1 years old). All procedures were performed with the animals under general anesthesia, adhered to the Association for Research in Vision and Ophthalmology's Statement for the Use of Animals in Ophthalmic and Vision Research, and were approved by the Institutional Animal Care and Use Committee at Legacy Research Institute. In all cases, anesthesia was induced with intramuscular ketamine (15 mg/kg) and xylazine (1.5 mg/kg), along with a single subcutaneous injection of atropine sulfate (0.05 mg/kg). Animals were intubated and breathed air spontaneously. Heart rate, end tidal CO_2, and arterial oxygenation saturation were monitored continuously (Propaq Encore model 206EL; Protocol Systems, Inc., Beaverton, OR). Body temperature was maintained with a heating pad at 37°C. Pupils were fully dilated with 1.0% tropicamide (Alcon Laboratories, Inc., Fort Worth, TX). One of the superficial branches of a tibial artery was cannulated with a 27-gauge needle, which was connected to a pressure transducer (BLPR2; World Precision Instruments [WPI], Inc., Sarasota, FL) and a four-channel amplifier system (Lab-Trax-4/24T; WPI). Arterial blood pressure (BP) was recorded continuously. Anesthesia was maintained by continuous administration of pentobarbital (6–9 mg/kg/h, IV) using an infusion pump (Aladdin; World Science Instruments, Inc., Sarasota, FL) in all procedures except during trabecular meshwork lasering sessions (see the following text).

IOP Measurement and RNFLT Imaging Protocol

IOP was measured by a handheld tonometer (Tono-Pen XL; Reichert, Inc., Depew, NY) in both eyes of each animal (mean of 3 measures per eye) within 30 minutes of general anesthesia induction. IOP in both eyes was manometrically controlled as described earlier.

Peripapillary RNFLT was measured in both eyes of each animal using a commercial spectral-domain optical coherence tomography (SD-OCT) instrument (Spectralis; Heidelberg Engineering GmbH, Heidelberg, Germany). For this study, the average peripapillary RNFLT was measured from a single circular B-scan consisting of 1536 A-scans. Nine to 16 individual sweeps were averaged in real time to comprise the final stored B-scan at each session. At the initial imaging session, the operator centered the position of the scan on the ONH (based on the view of the optic disc margin in the corresponding infrared reflectance image) and all subsequent scans were pinned (identical) to this location. A trained technician manually corrected the accuracy of the instrument's native automated layer segmentations when the algorithm had obviously erred from the inner and outer borders of the RNFL to an adjacent layer (such as a refractive element in the vitreous instead of the internal limiting membrane, or to the inner plexiform layer instead of the outer border of the retinal nerve fiber layer). All segmentations were then exported for extraction of RNFLT values by custom software.

Induction of Chronic Unilateral Experimental IOP Elevation

Laser treatment to one eye of each animal was performed under ketamine and xylazine anesthesia. In all, 180° of the trabecular meshwork (50-μm spot size, 1.0-second duration, 600- to 750-mW power) were treated in each of two separate sessions at least 2 weeks apart. Laser burns were calibrated to achieve blanching and bubbling of the meshwork without evident "pops" or bleeding. A sub-Tenon's injection of 0.5 mL of dexamethasone (10 mg/mL) was given in the inferior fornix of the treated eye. Laser treatments were repeated (but limited to a 90° sector) on multiple subsequent occasions as necessary to achieve sustained IOP elevation.

Blood Flow Measurement with LSFG

The principles of the LSFG technique (Softcare Ltd., Iizuka, Japan) and its application to measure ONH BF in nonhuman primates have been described in detail within previous publications.[27–30] In brief, a fundus camera equipped within the LSFG device was used to define an area centered on the ONH, with dimensions of approximately 3.8 × 3 mm (width × height). After switching on the laser ($\lambda = 830$ nm; maximum output power, 1.2 mW), a speckle pattern appears due to random interference of the scattered light from the illuminated tissue area, which is continuously imaged by a charge-coupled device (700 × 480 pixels) at a frequency of 30 frames per second for 4 seconds at a time.

Offline analysis software computed the mean blur rate (MBR) of the speckle images. MBR is a squared ratio of mean intensity to the SD of light intensity, which varies temporally and spatially according to the velocity of blood cells' movement and correlates well with capillary BF within the ONH.[27,31] A composite MBR map representing BF distribution within the ONH disc was generated from the images of each 4-second series. After eliminating the area within the images corresponding to large blood vessels, capillary BF within the remaining ONH disc area was averaged and recorded in arbitrary units (AU) of MBR.

BF Measured with the Microsphere Method

Under general anesthesia, both femoral arteries and a vein were cannulated with polyethylene tubes (PE50) for BP monitoring, reference blood sample collection (see the following text), and administration of drugs, respectively. The left ventricle was cannulated via the right brachial artery with the same type of polyethylene tubing. Once arterial BP and end-tidal PCO_2 were stabilized within normal ranges, 60 million fluorescent microspheres (PolySciences, Inc., Warrington, PA) with a 10-μm diameter, suspended in a solution of 5 mL of 0.15 M NaCl and 0.05% Tween 20, were injected into the left ventricle over a period of 25 to 45 seconds after heparinizing the blood (500 IU/kg, IV). Note that in two male monkeys with larger body weight, 100 million microspheres were injected. A reference blood sample was drawn from one of the cannulated arteries, starting from the onset of microsphere injection, for 1 or 2 minutes. Animals were then euthanized by overdose of intravenous pentobarbital (Euthasol; Delmarva Laboratories, Inc., Midlothian, VA), then both eyes were enucleated and postfixed in 4% paraformaldehyde for 48 hours, after which they were embedded in optimal cutting temperature (O.C.T.) compound (Tissue-Tek O.C.T. Compound; Sakura Finetek USA, Inc., Torrance, CA).

For each embedded eye, consecutive serial longitudinal frozen sections were obtained by a cryostat with 25 μm thickness. These sections were collected on a series of numbered glass slides and air dried. The microsphere concentration in the reference blood was determined in a hemacytometer (Fuchs–Rosenthal Counting Chamber;

Table. RNFLT and Interocular BF Difference (%) Measured by LSFG and the Microsphere Method

			Microsphere Method			
ID	**RNFLT Loss**	**LSFG-BF**	**MS-BF$_{ANT}$**	**MS-BF$_{POST}$**	**MS-BF$_{A+P}$**	**MS-BF$_{PP}$**
135	−31%	−24%	−24%	−25%	−25%	*
136	−35%	−33%	−25%	−59%	−48%	−27%
137	−6%†	−11%	−21%	−18%	−19%	*
139	−38%	**9%**	−60%	**30%**	**11%**	−6%
140	−37%	−25%	−55%	−21%	−28%	−30%
25340	−44%	−22%	−28%	−45%	−42%	−43%
25904	−59%	−27%	−42%	−43%	−43%	−39%
28506	−56%	−32%	−50%	**35%**	**18%**	−33%
28849	−62%	−29%	−64%	−50%	−52%	−31%
Mean	−42%	−22%	−41%	−22%	−25%	−30%
SD	16%	13%	17%	34%	25%	12%

* Peripapillary retinal tissues were not available.

† This experiment was terminated before endpoint due to development of cataract.

Electron Microscopy Sciences, Hatfield, PA). Each ONH section was photographed with a 10× lens under a fluorescent microscope equipped with an automated imaging system. Montages of the photographs for each ONH section were created digitally. The total microspheres within a given region of ONH (see the following text) were counted. With the microsphere counts in both reference blood and ONH, total BF in a given defined region (μL/min) was calculated as: N_{tissue}/C_{ref}, where N_{tissue} was the microsphere count in the tissue of interest and C_{ref} is the microsphere number per μL reference blood per minute.

The ONH BF was determined for two layers (depth regions) divided by the posterior border of the lamina cribrosa: the first layer included the superficial NFL, prelaminar tissue, and lamina cribrosa (anterior ONH); the second layer included the first 1 mm of the retrolaminar optic nerve (posterior ONH). BF in the peripapillary retina was also measured in seven pairs of the eyes from an annulus of tissue obtained by two trephine cuts (6 and 2.5 mm) centered on the optic disc. The number of microspheres within this 23.4 mm^2 peripapillary annulus of retina was counted and BF was calculated using the same method as described earlier for ONH BF.

Experiment Protocol

Three to five baselines of IOP, RNFLT, and LSFG-BF were acquired from both eyes of each animal. EG was then induced by laser treatment to one eye of each animal to induce chronic IOP elevation. The IOP, RNFLT, and LSFG-BF measurements were then repeated biweekly following the onset of laser treatment to induce IOP elevation until RNFLT in the EG eye had declined by approximately 40% of the baseline average. A final BF measurement was then performed by LSFG and the microsphere method on the day when the animal was euthanized. In six of the nine animals, the last LSFG BF measurement was followed immediately by the microsphere BF measurement. In two animals, the LSFG-BF was measured 4 and 7 days prior to the microsphere method, respectively. In one animal (ID 28506), the last LSFG-BF measurement was measured 43 days earlier than that measured by the microsphere method due to development of cataract in the control eye, thus preventing clear in vivo imaging. All BF measurements by both LSFG and the microsphere method were performed at least 5 minutes after IOP had been manometrically set at 40 mm Hg.

Statistics

All data were reported as mean ± SD. Statistical analysis was performed using commercially available software (Prism V 5.0.4; SoftPad Software, Inc., La Jolla, CA). Paired Student's *t*-tests were used to evaluate the mean BF difference between the eyes and between baseline and final measurements within eyes. Linear regression was used to correlate the interocular BF differences measured by LSFG and the microsphere method. Probability <5% was considered as the critical level for rejecting the null hypothesis.

Results

IOP and RNFLT

Average postlaser IOP in the EG eyes was 30 ± 6 vs. 13 ± 2 mm Hg in the contralateral controls ($P < 0.001$). The highest IOP recorded in the EG eyes averaged 46 ± 7 mm Hg, ranging from 35 to 57 mm Hg and the total duration of elevated IOP was 4.8 ± 2.6 months, ranging from 1 to 10 months. Baseline RNFLT showed no difference between the two eyes of each animal ($P = 0.69$). RNFLT loss in the EG eye relative to prelaser baseline values was 42 ± 16% on average ($P = 0.0001$), ranging from 6% to 59% at the end of last data collection, with one animal being terminated before the endpoint due to development of a cataract in the control eye.

LSFG BF Measurement

Mean baseline LSFG-BF was 11.1 ± 1.4 (AU) in the EG eyes versus 10.8 ± 1.4 in the fellow control eyes ($P = 0.43$). Mean EG eye LSFG-BF at the last imaging session was 9.2 ± 1.7 (AU) versus 11.7 ± 1.9 in the contralateral control eyes ($P = 0.003$), corresponding to a 22 ± 13% reduction (Table). In one of the EG eyes, the LSFG-BF was 9% higher than that in the contralateral control eye. This EG eye was also one of the two EG eyes with increased BF in the posterior ONH (see the following text and Table).

Longitudinal comparison of LSFG-BF between baseline and the endpoint showed no significant difference in the control eyes ($P = 0.20$), but the LSFG-BF was significantly reduced at the endpoint in EG eyes ($P = 0.01$).

Figure 1 illustrates the baseline and the final time point of optic disc photographs, peripapillary RNFLT measured by SD-OCT, and LSFG MBR composite maps in both eyes of a representative experimental animal (ID 28849).

BF Measurement with the Microsphere Method

BP during the BF Measurement. Average mean BP was 93.2 ± 9.9 mm Hg immediately prior to microsphere injection. During injection (duration of 1 or 2 minutes), mean BP either did not change ($n = 5$) or decreased transiently by <10 mm Hg

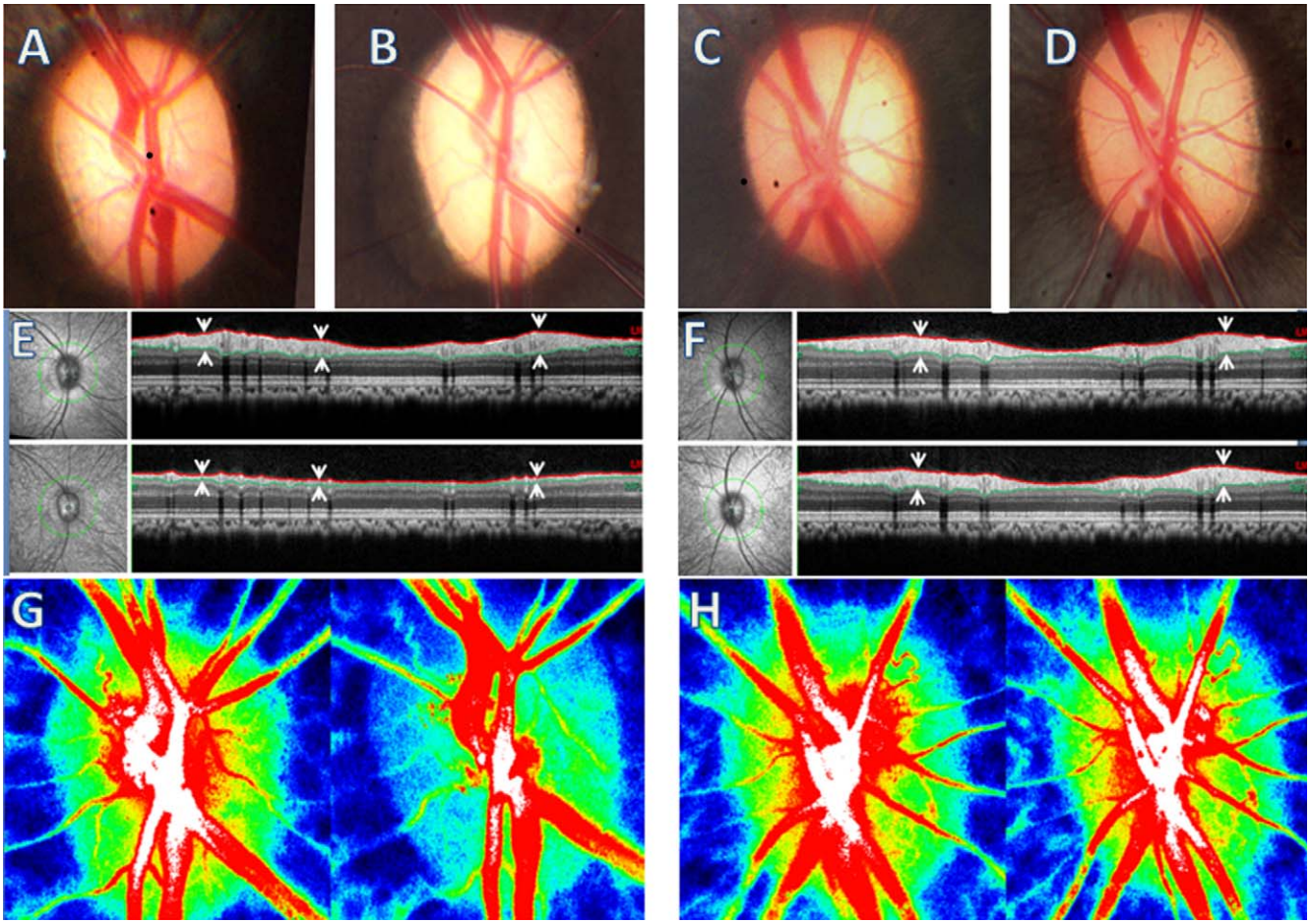

Figure 1. *Left panels*: Example of EG eye. *Right panels*: The fellow control eye. The average IOP in the EG eye was 30 mm Hg and 17 mm Hg in the control eye during the 4.5-month period of IOP elevation. The fundus photograph in the EG eye at the last time point examination (**B**) shows optic disc pallor compared with its baseline (**A**); there was no change in the control eye [**C**] versus [**D**]. The photograph on the *left* of (**E**) and (**F**) show the infrared image of the fundus. The peripapillary *green circles* show the path of the B-scan from which the RNFLT is measured (*right*). The RNFLT in the EG eye (**E**) was reduced by 62% at the final time point (*lower panel*) from baseline (*upper panel*); there was no RNFLT change in the control eye (**F**). RNFLT is marked by the *paired arrows*, which point to the anterior and posterior borders, and marked with *red* and *green lines*, respectively. (**G**, **H**) ONH LSFG MBR composite maps measured at baseline (*left*) and final time point (*right*), respectively. The BF is encoded with pseudocolor from high (*red*) to low (*blue*). Note the superotemporal ONH BF at the final time point in the EG eye ([**G**], *right*) is lower compared with baseline ([**G**], *left*), which represents 29% of overall ONH BF decrease.

(mean ± SD: 7.8 ± 2.6, $n = 4$) and then returned to its preinjection level within approximately 10 to 20 seconds. At the end of the injection, the average mean BP was 91.3 ± 11.1 mm Hg. Since the IOP was set at 40 mm Hg in both eyes during the BF measurement, the corresponding ocular perfusion pressure (OPP) was 45 mm Hg less than the mean BP. The 5 mm Hg differential reflects a correction for the height difference between the tested eye and the level where BP was measured.

BF in the Anterior and Posterior ONH (Figs. 2B–D). In control eyes, the average MS-BF_{ANT} was 1.37 ± 0.56 μL/min and in EG eyes it was 0.88 ± 0.54 μL/min ($P < 0.0001$, paired Student's *t*-test; Fig. 2B). The reduction in MS-BF_{ANT} corresponded to a 41 ± 17% in the EG eyes relative to their fellow control eyes (Table). Average MS-BF_{POST} was 4.60 ± 1.1 μL/min in control eyes and 3.45 ± 1.4 μL/min in EG eyes ($P = 0.064$), representing a 22 ± 34% reduction in EG eyes (Fig. 2C, Table). Although the overall trend was similar to MS-BF_{ANT}, the EG MS-BF_{POST} reduction was complicated by the fact that two EG eyes demonstrated an increase rather than a decrease (Table). The combined BF of both anterior and posterior ONH (MS-BF_{A+P}) was 5.98 ± 1.5 μL/min in control eyes and 4.32 ± 1.4 in EG eyes ($P = 0.016$, Fig. 2D), representing a 25 ± 25% reduction in the EG eyes relative to their fellow control eyes (Table).

BF in the Peripapillary Retina (Fig. 1E). Total BF in the 23.4 mm^2 peripapillary annulus of retina (MS-BF_{PP}) was 3.11 ± 0.85 μL/min in control eyes and 2.17 ± 0.63 μL/min in EG eyes ($P = 0.001$, $n = 7$). This difference represented a 30 ± 12% reduction in EG eyes relative to fellow controls (Table).

The Table lists the RNFLT changes measured by SD-OCT (column 2) and interocular BF difference (%) in each pair of the eyes measured by the LSFG (column 3) and by the microsphere method (columns 4–7). Note that the MS-BF_{ANT} values in all EG eyes were reduced (column 4). The average MS-BF_{POST} (column 5) was also reduced in EG eyes except in two of the nine eyes, in which the MS-BF_{POST} was 30% and 35% higher than that in their fellow control eyes (see numbers in bold in Table). The combined BF (BF_{A+P}, column 6) showed similar change to the MS-BF_{POST}.

In the two EG eyes (ID 139 and ID 28506) with increased MS-BF_{POST} as measured by the microsphere method, one of them (ID 139) showed 9% higher LSFG-BF as well. The other EG eye with higher MS-BF_{POST} (ID 28506), had lower LSFG-BF

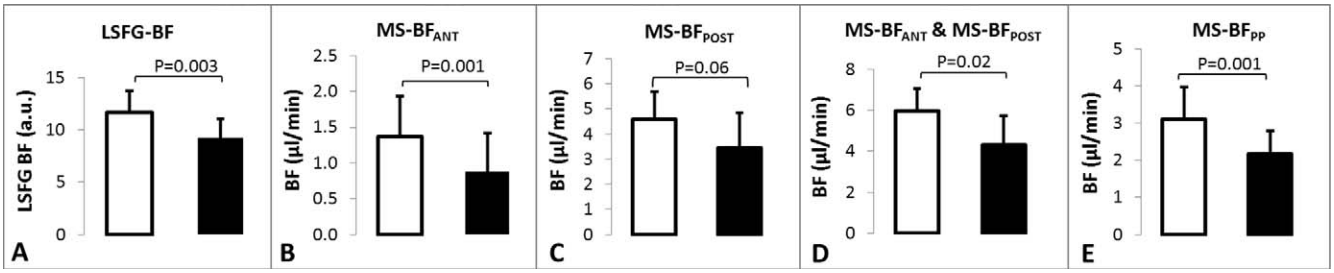

Figure 2. BF in EG (*black columns*) and contralateral control eyes (*white columns*) measured by LSFG (**A**) and by the microsphere method (**B**–**E**). (**B**) Anterior ONH. (**C**) Posterior ONH. (**D**) Total BF in combined anterior and posterior ONH. (**E**) Peripapillary retina. Error bars = ±SD.

measured 42 days earlier than the microsphere method measurement.

Correlation of Interocular BF Difference Measured by LSFG and the Microsphere Method

LSFG and Microsphere BF data for eight of the nine animals were included in this analysis. Animal 28506 was excluded because the last available LSFG BF measurement occurred 42 days prior to euthanization (and its associated microsphere measurement). As shown in Figure 3, interocular BF differences measured by LSFG correlated significantly to microsphere MS-BF$_{POST}$ ($R^2 = 0.88$; $P < 0.001$) and MS-BF$_{A+P}$ ($R^2 = 0.87$; $P < 0.001$; Figs. 3B, 3C, respectively), but not with MS-BF$_{ANT}$ ($R^2 = 0.051$, $P > 0.05$; Fig. 3A) in these eight eyes.

Discussion

In the current study, compromised BF in the anterior ONH of EG eyes was demonstrated in nonhuman primates' EG measured by both LSFG and the microsphere method. Compromised BF in the retrolaminar region was also demonstrated by the microsphere method, which enables evaluation of BF within specific depths of the ONH. The high correlation between the BF reduction in the posterior ONH but not anterior ONH measured by LSFG and that measured by the microsphere method provides evidence that the LSFG technique is capable of assaying BF for a critical region of the ONH, which served primarily by the short posterior ciliary circulation (and recurrent pial branches).

Increased IOP is one of the major risk factors associated with glaucomatous optic neuropathy including structural damage and likely also compromised microcirculation within the ONH. Biomechanical alterations of glaucoma within the ONH tissues is a topic of extensive investigation.[32] The effect of glaucoma on ONH microcirculation, however, remains inconclusive. One of the longstanding questions about glaucomatous optic neuropathy is whether reduced BF is a preexisting pathologic change or a consequence of glaucomatous optic atrophy.[33,34] This has been difficult to determine in part because a substantial portion of retinal ganglion cells/axons may have already become degenerated even at an "early" clinical stage of glaucoma.[35,36] Previous studies in experimental models of glaucoma based on chronic IOP elevation failed to show significant BF changes probably because of either low sensitivity of the methods used to measure blood flow[37,38] or/and insufficient statistical power.[39] In the current study, the EG eyes had undergone approximately 5 months of chronic IOP elevation and achieved 42% RNFLT loss on average at the time of the microsphere BF measurement. The percentage of retinal ganglion cell/axon loss in the ONH was likely even higher, approaching approximately 60%,[40] suggesting that the reduced BF detected in the glaucomatous ONH could be, at least in part, a result of ONH degeneration and consequently diminished metabolic demand.

Interestingly, the ONH BF was not reduced uniformly in depth as demonstrated by the microsphere method. Although all EG eyes had reduced MS-BF$_{ANT}$ and the majority of the EG eyes had reduced MS-BF$_{POST}$, two of the nine EG eyes in fact had higher MS-BF$_{POST}$ (see Table). This hyperemic response was also observed during earlier stages measured by LSFG in additional EG eyes (results of "staging" analyses; i.e., longitudinal LSFG versus RNFLT will be the subject of a separate communication). Previous studies by Quigley et al.[37] showed similarly mixed BF changes between individual animals and

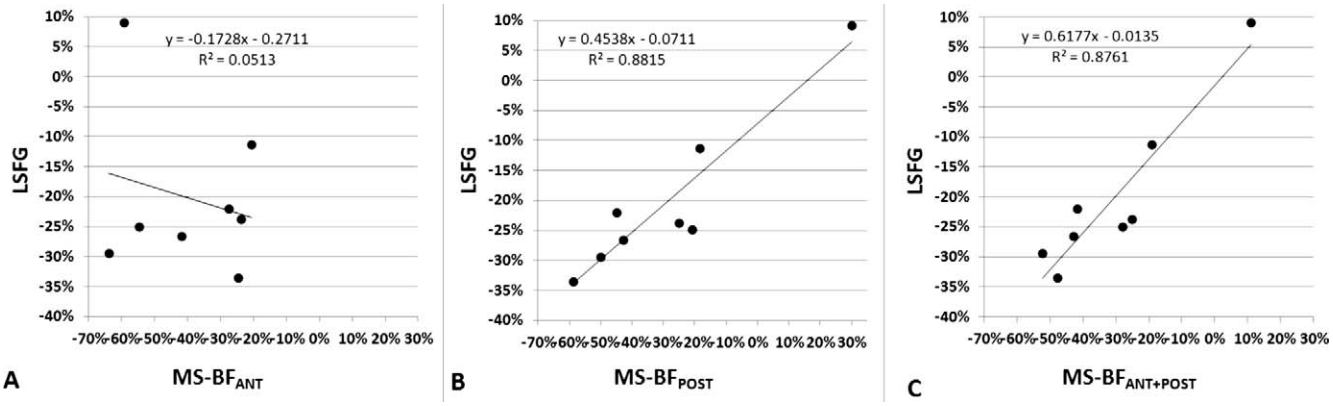

Figure 3. Linear regression analysis shows the correlation of interocular BF differences in the anterior ONH (**A**), posterior ONH (**B**), and the combined anterior and posterior ONH (**C**) measured by LSFG (*y*) and microsphere method (*x*). Note the outlier in (**A**) (*top left corner*) was one of the two eyes with high MS-BF$_{POST}$ (ID 139 in Table).

ONH depths, with an overall slight decrease of BF in the anterior ONH and a slight increase of BF in the retrobulbar (posterior) ONH in nonhuman primate EG models, suggesting that during any given stage of EG, the vasculature in the posterior ONH may develop temporary hyperemia. This may explain, at least in part, the insignificant BF change in the two previous studies[37,39] and perhaps also contradictory results of BF studies in human glaucoma.[41]

In the current study, the ONH BF was measured at IOP set at 40 mm Hg in both eyes. At this IOP, no BF change was expected in control eyes because the corresponding OPP was close to, but above, the lower limit of autoregulation in the ONH (Wang L, et al. *IOVS* 2012;53:ARVO E-Abstract 6851). In the EG eyes, since the OPP was just above the margin of the lower limit of autoregulation, the BF was more likely to be compromised if the autoregulation had failed. Thus, in addition to the structural damage, impaired autoregulation may also be one of the possible mechanisms contributing to the reduced BF observed in EG eyes.

Although compromised ONH BF was demonstrated in EG eyes both by the microsphere method and by LSFG, each of these methods has certain limitations. When BF is measured by the microsphere method in small volume tissues, such as the ONH, the number of microspheres entrapped within the tissue is small, which may cause larger measurement variation. For this reason, we counted all three superficial ONH layers together (anterior ONH) to maximize the total microsphere numbers. Nevertheless, these numbers were still below the number typically recommended for tissue BF measurement.[42] However, the relatively large effect size (i.e., the 25% BF difference between EG and control eyes) strengthened the statistical power and overcame the relatively small tissue volume, as has been observed in previous studies.[43–45] Another limitation of the microsphere method in this study was the potential that the volume of tissue was reduced by the significant degree of neurodegeneration, which could result in fewer microspheres counted, irrespective of BF density within the tissue volume. The LSFG technique measures BF for the capillaries within an approximately fixed volume of tissue (i.e., effectively the capillary blood flow "density"), so the lower LSFG-BF and the strong correlation between LSFG-BF and BF measured by the microsphere technique would suggest that the capillary BF reduction in EG eyes was the dominant factor over potential reduction of tissue volume.

The laser speckle imaging technique also has certain limitations. It is thought that since the parameters of the calibration equation (i.e., its constant and zero offset) used to calculate the blur rate of speckle images are derived from in vitro tests, the assumption that they may be appropriate for all tissues with varying light absorbance/scattering properties may be flawed.[27] For example, large differences in the absorbance/scattering properties exist between myelinated and nonmyelinated regions of retina such that the LSFG measures in these areas might not be comparable.[20] For the same reason, tissue properties may also differ under pathologic conditions, although this has never been verified. Thus, it has been recommended that BF comparisons between tissues with different properties should be avoided.[27] In the current study, the BF comparison was restricted to the same tissue type (i.e., ONH). Under such a condition, the LSFG-BF between the pairs of eyes showed no difference prior to lasering. It was significantly decreased in EG eyes after chronic IOP elevation. Because the ONH in EG eyes at the endpoint had undergone significant tissue degeneration, it might be the tissue property change that contributed to the blur rate change, at least in part, rather than being strictly reflective of BF changes. However, this is not likely because, as the results of the current study demonstrated, the BF change measured by LSFG was strongly correlated with that measured by the microsphere method. Moreover, if the decreased blur rate in EG eyes was predominantly caused by tissue property changes, the blur rate would be expected to change uniformly in all EG eyes (either all increasing or all decreasing) in conjunction with the relatively uniform degree of neurodegeneration (e.g., as measured by RNFLT), regardless of whether the BF increased or decreased in these eyes. On the contrary, in several of the EG eyes with significantly reduced RNFLT, increased BF was observed for both LSFG and for the posterior ONH measured by the microsphere method. Together, the results of the current study leave little doubt that the potential confound on calculated blur rate caused by tissue degeneration, if any, is much smaller compared with the dominant signals derived from actual BF changes.

The results of this study also suggest that the MBR scale for LSFG (in AU) is compressed relative to BF measured by the microsphere technique. For example, the interocular LSFG-BF differences were smaller compared with that measured by the microsphere method as shown in Figure 3. This smaller interocular LSFG-BF difference is likely a result of error in the MBR calibration parameters having been derived from in vitro studies as mentioned earlier. Ongoing studies are being conducted to address at least the offset parameter for the LSFG calibration in vivo.

Notwithstanding these technical limitations, the present study demonstrated two important observations: the first is significantly reduced BF in the ONH after chronic IOP elevation measured by two independent techniques; the second is a strong correlation of BF measurement between the LSFG and the microsphere method. These findings provide experimental evidence of direct association between chronic IOP elevation and impaired ONH microcirculation, and validate the BF measurement by LSFG in ONH with experimentally glaucomatous neural degeneration.

References

1. Chiba N, Omodaka K, Yokoyama Y, et al. Association between optic nerve blood flow and objective examinations in glaucoma patients with generalized enlargement disc type. *Clin Ophthalmol*. 2011;5:1549–1556.
2. Hamard P, Hamard H, Dufaux J. Blood flow rate in the microvasculature of the optic nerve head in primary open angle glaucoma. A new approach. *Surv Ophthalmol*. 1994;38: S87–S94.
3. Hayreh SS. The 1994 Von Sallman Lecture. The optic nerve head circulation in health and disease. *Exp Eye Res*. 1995;61: 259–272.
4. Yokoyama Y, Aizawa N, Chiba N, et al. Significant correlations between optic nerve head microcirculation and visual field defects and nerve fiber layer loss in glaucoma patients with myopic glaucomatous disk. *Clin Ophthalmol*. 2011;5:1721–1727.
5. Cioffi GA. Three common assumptions about ocular blood flow and glaucoma. *Surv Ophthalmol*. 2001;45(suppl 3): S325–S331; discussion S332–S334.
6. Hayreh SS. Evaluation of optic nerve head circulation: review of the methods used. *J Glaucoma*. 1997;6:319–330.
7. Harris A, Kagemann L, Cioffi GA. Assessment of human ocular hemodynamics. *Surv Ophthalmol*. 1998;42:509–533.
8. Hayreh SS. Anatomy and physiology of the optic nerve head. *Trans Am Acad Ophthalmol Otolaryngol*. 1974;78:OP240–OP254.
9. Hayreh SS. Blood supply of the optic nerve head. *Ophthalmologica*. 1996;210:285–295.

10. Laties AM. Central retinal artery innervation. Absence of adrenergic innervation to the intraocular branches. *Arch Ophthalmol*. 1967;77:405–409.
11. Ye XD, Laties AM, Stone RA. Peptidergic innervation of the retinal vasculature and optic nerve head. *Invest Ophthalmol Vis Sci*. 1990;31:1731–1737.
12. Cioffi GA. Vascular anatomy of the anterior optic nerve. In: Pillunat LE, Harris A, Anderson DR, Greve EL, eds. *Current Concepts on Ocular Blood Flow in Glaucoma*. The Hague: Kugler Publications; 1999:45–52.
13. Petrig BL, Riva CE, Hayreh SS. Laser Doppler flowmetry and optic nerve head blood flow. *Am J Ophthalmol*. 1999;127: 413–425.
14. Petrig BL, Riva CE, Hayreh SS. Optic nerve blood flow in the rhesus monkey measured by laser Doppler flowmetry. *Noninvasive Assessment of the Visual System: Technical Digest Series,* Vol. 1. Washington, DC: Optical Society of America; 1992:114–117.
15. Koelle JS, Riva CE, Petrig BL, Canstoun SD. Depth of tissue sampling in the optic nerve head using laser Doppler flowmetry. *Lasers Med Sci*. 1993;8:49–54.
16. Wang L, Cull G, Cioffi GA. Depth of penetration of scanning laser Doppler flowmetry in the primate optic nerve. *Arch Ophthalmol*. 2001;119:1810–1814.
17. Sehi M. Basic technique and anatomically imposed limitations of confocal scanning laser Doppler flowmetry at the optic nerve head level. *Acta Ophthalmol*. 2011;89:e1–e11.
18. Rival R, Bance M, Antonyshyn O, Phillips J, Pang CY. Comparison of laser Doppler flowmeter and radioactive microspheres in measuring blood flow in pig skin flaps. *Laryngoscope*. 1995;105:383–386.
19. Tamaki Y, Araie M, Fukaya Y, Ishi K. Validation of scanning laser Doppler flowmetry for retinal blood flow measurements in animal models. *Curr Eye Res*. 2002;24:332–340.
20. Tamaki Y, Araie M, Kawamoto E, Eguchi S, Fujii H. Noncontact, two-dimensional measurement of retinal microcirculation using laser speckle phenomenon. *Invest Ophthalmol Vis Sci*. 1994;35:3825–3834.
21. Geijer C, Bill A. Effects of raised intraocular pressure on retinal, prelaminar, laminar, and retrolaminar optic nerve blood flow in monkeys. *Invest Ophthalmol Vis Sci*. 1979;18: 1030–1042.
22. Aizawa N, Yokoyama Y, Chiba N, et al. Reproducibility of retinal circulation measurements obtained using laser speckle flowgraphy–NAVI in patients with glaucoma. *Clin Ophthalmol*. 2011;5:1171–1176.
23. Cheng H, Duong TQ. Simplified laser-speckle-imaging analysis method and its application to retinal blood flow imaging. *Opt Lett*. 2007;32:2188–2190.
24. Mayama C, Ishii K, Saeki T, Ota T, Tomidokoro A, Araie M. Effects of topical phenylephrine and tafluprost on optic nerve head circulation in monkeys with unilateral experimental glaucoma. *Invest Ophthalmol Vis Sci*. 2010;51:4117–4124.
25. Nagahara M, Tamaki Y, Tomidokoro A, Araie M. In vivo measurement of blood velocity in human major retinal vessels using the laser speckle method. *Invest Ophthalmol Vis Sci*. 2011;52:87–92.
26. Sugiyama T, Utsumi T, Azuma I, Fujii H. Measurement of optic nerve head circulation: comparison of laser speckle and hydrogen clearance methods. *Jpn J Ophthalmol*. 1996;40: 339–343.
27. Sugiyama T, Araie M, Riva CE, Schmetterer L, Orgul S. Use of laser speckle flowgraphy in ocular blood flow research. *Acta Ophthalmol*. 2010;88:723–729.
28. Fujii H, Nohira K, Yamamoto Y, Ikawa H, Hjura T. Evaluation of blood flow by laser speckle image sensing. Part 1. *Applied Optics*. 1987;26:5321–5325.
29. Liang Y, Downs JC, Fortune B, Cull G, Cioffi GA, Wang L. Impact of systemic blood pressure on the relationship between intraocular pressure and blood flow in the optic nerve head of nonhuman primates. *Invest Ophthalmol Vis Sci*. 2009;50:2154–2160.
30. Liang Y, Fortune B, Cull G, Cioffi GA, Wang L. Quantification of dynamic blood flow autoregulation in optic nerve head of rhesus monkeys. *Exp Eye Res*. 2010;90:203–209.
31. Takayama J, Tomidokoro A, Ishii K, et al. Time course of the change in optic nerve head circulation after an acute increase in intraocular pressure. *Invest Ophthalmol Vis Sci*. 2003;44: 3977–3985.
32. Burgoyne CF, Downs JC, Bellezza AJ, Suh JK, Hart RT. The optic nerve head as a biomechanical structure: a new paradigm for understanding the role of IOP-related stress and strain in the pathophysiology of glaucomatous optic nerve head damage. *Prog Retin Eye Res*. 2005;24:39–73.
33. Flammer J, Orgul S, Costa VP, et al. The impact of ocular blood flow in glaucoma. *Prog Retin Eye Res*. 2002;21:359–393.
34. Pournaras CJ, Riva CE, Bresson-Dumont H, De Gottrau P, Bechetoille A. Regulation of optic nerve head blood flow in normal tension glaucoma patients. *Eur J Ophthalmol*. 2004; 14:226–235.
35. Harwerth RS, Crawford ML, Frishman LJ, Viswanathan S, Smith EL III, Carter-Dawson L. Visual field defects and neural losses from experimental glaucoma. *Prog Retin Eye Res*. 2002;21:91–125.
36. Kerrigan-Baumrind LA, Quigley HA, Pease ME, Kerrigan DF, Mitchell RS. Number of ganglion cells in glaucoma eyes compared with threshold visual field tests in the same persons. *Invest Ophthalmol Vis Sci*. 2000;41:741–748.
37. Quigley HA, Hohman RM, Sanchez R, Addicks EM. Optic nerve head blood flow in chronic experimental glaucoma. *Arch Ophthalmol*. 1985;103:956–962.
38. Caprioli J, Miller JM. Measurement of optic nerve blood flow with iodoantipyrine: limitations caused by diffusion from the choroid. *Exp Eye Res*. 1988;47:641–652.
39. Alm A, Lambrou GN, Maepea O, Nilsson SF, Percicot C. Ocular blood flow in experimental glaucoma: a study in cynomolgus monkeys. *Ophthalmologica*. 1997;211:178–182.
40. Cull GA, Reynaud J, Wang L, Cioffi GA, Burgoyne CF, Fortune B. Relationship between orbital optic nerve axon counts and retinal nerve fiber layer thickness (RNFLT) measured by spectral domain optical coherence tomography. *Invest Ophthalmol Vis Sci*. 2012;53:7766–7773.
41. Hollo G, van den Berg TJ, Greve EL. Scanning laser Doppler flowmetry in glaucoma. *Int Ophthalmol*. 1996;20:63–70.
42. Buckberg GD, Luck JC, Payne DB, Hoffman JI, Archie JP, Fixler DE. Some sources of error in measuring regional blood flow with radioactive microspheres. *J Appl Physiol*. 1971;31:598–604.
43. Ahmed J, Pulfer MK, Linsenmeier RA. Measurement of blood flow through the retinal circulation of the cat during normoxia and hypoxemia using fluorescent microspheres. *Microvasc Res*. 2001;62:143–153.
44. Lin J, Roth S. Ischemic preconditioning attenuates hypoperfusion after retinal ischemia in rats. *Invest Ophthalmol Vis Sci*. 1999;40:2925–2931.
45. Wang L, Fortune B, Cull G, McElwain KM, Cioffi GA. Microspheres method for ocular blood flow measurement in rats: size and dose optimization. *Exp Eye Res*. 2007;84:108–117.